Approach to Automatic Segmentation of Atherosclerotic Plaque in B-images Using Active Contour Algorithm Adapted by Convolutional Neural Network to Echogenicity Index Computation

Jiri Blahuta, Tomas Soukup, Petr Sosik

Silesian University in Opava, The Department of Computer Science, Opava, Czech Republic

Abstract: The presented paper is dedicated to image processing of ultrasound B-images in neurosonology. Atherosclerotic plaques in in-vitro B-images are analyzed in this study. The content is divided into two core parts.

The first one is focused on computing Echo-Index value inside the atherosclerotic plaque as a defined Region of Interest. From achieved results is obvious that the Echo-Index is well-reproducible value in general. Totally of 278 images were analyzed by two non-experienced observers and by an experienced sonographer to validate the result. Basic statistical descriptors were calculated to judge the level of agreement. In this part, the ROI were selected manually.

The second part is focused on approach to automatic selection of the ROI. Manual drawing of the border is time-consuming. Our idea is to use active contour algorithm (ACM; Active Contour Model) to eliminate the black background from the displayed plaque. Using ACM can be useful way to select ROI automatically. The main issue is to separate the shape of the plaque from neighbor structures, especially from the bottom of the tube. To adapt ACM, the principle of the convolutional neural network can be used to extract the feature of the shape to select a correct ROI. Thus, CNN can be trained and learnt to adapt number of iterations of the ACM (or another parameter) based on supervised learning from properly bordered examples. The main disadvantage is time-consuming process and high performance to be needed to train and learn the CNN. In fact, in this study, there is no real design of CNN but the primary goals are defined to realize in future.

1 Motivation and Input Data

In recent few decades, ischemic stroke caused by atherosclerosis is one of the top causes of the mortality worldwide. In modern neurology, ultrasound B-imaging is one of the diagnostic tools to detect atherosclerotic plaques in general. The diagnostic ultrasound [1] is a fast, non-invasive examination which is also combined with another modalities, such as CT or MRI. The atherosclerotic plaques are well displayed in B-image but the limitation is to understand their complex structure to find some markers to predict severe problems. Increased echogenicity of the plaque can be one of the detectable features as well. Principles and methods of neurosonology are described in [2].

In 2011, we developed a software tool *B-MODE Assist* using binary thresholding algorithm to detect hyperechogenicity of the substantia nigra. Due to general properties of B-images in grayscale, the software can be used also for the atherosclerotic plaques but in slightly adapted form.

1.1 Input B-images

For this research, a set of 278 B-images (in-vitro) is processed. In Fig. 1, an example of the B-image in which the plaque is displayed, is stated.

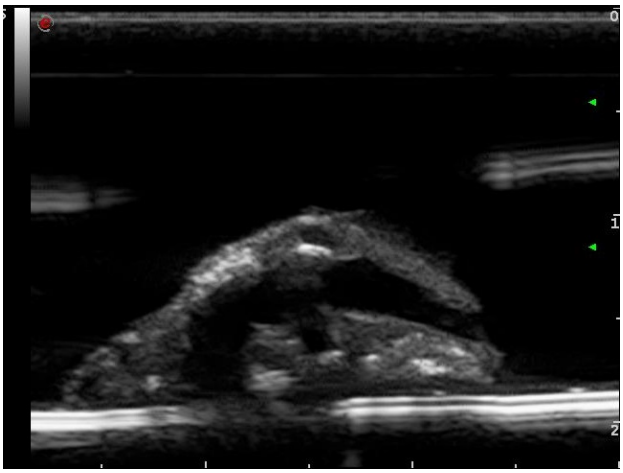

Figure 1: Input B-image with atherosclerotic plaque in-vitro

Our recent research has been based on computing the echogenicity index (called Echo-Index) to comparison of the risk of the plaque using our developed software and a visual assessment by an experienced sonographer.

2 Echogenicity Index in A Free-Hand ROI

The echogenicity index (Echo-Index) is one numeric value which could corresponds with the echogenicity grade. The Echo-Index is computed in closed Region of Interest, in this case in the atherosclerotic plaque. To obtain the Echo-Index, we use own developed software tool B-MODE Assist, originally developed for substantia nigra echogenic

area computation. Hyperechogenic substantia nigra is a detectable parkinsonic marker in B-image. The algorithm is fully described in our previous publications, e.g. [3] and [6]. The important clinical study based on this software have been published in 2014 [4] and [6]. The basic principle can be described by the following steps:

1. Load an input image (in bitmap or DICOM format) which is converted into 8-bit grayscale depth automatically
2. Select a window in which the examined structure is shown, i.e. atherosclerotic plaque
3. Select a Region of Interest (in the case of atherosclerotic plaques, ROI of a free shape); the ROI is a binary mask
4. Inside the ROI, the area is computed according to threshold
   (a) The area is computed as the number of remaining pixels after binary thresholding algorithm
   (b) For each threshold T in the range of 0 to 255, the number of pixels is computed
   (c) The number of pixels is converted into real mm^2 according to displayed scale, i.e. the window size in step 2 (the size of 20×20 mm is used)
5. All values of the area for all 256 thresholds are drawn as a "curve" (256 isolated values); see Fig. 2.

In the case of analysis of the substantia nigra, this algorithm was genuinely useful. The speed of decreasing of the area inside the ROI has been observed. For substantia nigra, an equal shape of the ROI is used; an elliptical shape with area of 50 mm^2. It was sufficient for clinical studies, e.g. [5] to statistical analysis of the echogenicity grade of the substantia nigra.

In the case of atherosclerotic plaques, the main difference is the fact that ROI is selected by a free-hand shape and the area is different for each plaque. In Fig. 2, six different shapes of the plaque are presented as a closed ROI selected in the window 20×20 mm.

The idea of the Echo-Index is considered as a number which can describe echogenicity grade inside the plaque; inside the free-hand ROI. Let H is the brightness value of a pixel and T to be the threshold then A_T is the computed area for each threshold T in the range of $0 \leq T \leq 255$. The sum is computed

$$AREASUM = \sum_{T=0}^{255} A_T \tag{1}$$

and the $AREASUM$ value is divided by 100

$$EchoIndex = \frac{AREASUM}{100} \tag{2}$$

and this value we called Echo-Index.

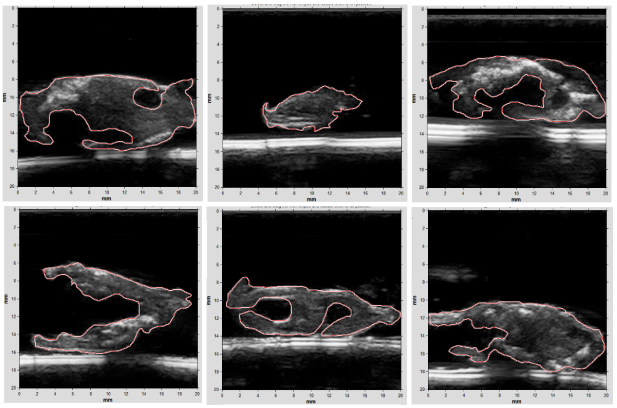

Figure 2: Six different shapes of the plaque in in-vitro B-images

Due to the principle of binary thresholding, for lower echogenicity grade, the Echo-Index should be lower and for higher echogenicity the Echo-Index should be higher. This is an assumption which proceeds from the principle of binary thresholding. Thus, in the case of low echogenicity, for low T threshold the computed area should be very low and vice versa. In consequence of this principle, the sum for low echogenicity is low and for high echogenic ROI the sum is higher. During the future work it should be confirmed whether this idea is correct or not; especially in comparison with visual assessment.

2.1 General Reproducibility Assessment of the Echo-Index

The goal of the pilot study [8] was to prove the reproducibility of the index; total of 284 B-images were analyzed using this software with this following conditions:

- 2 independent non-experienced observers measured all images two times
- each observer measured for 2 weeks; for one week the first has been performed (278 images) and for following week the second measuring has been performed (the same set of 278 images)
- all images have the same resolution but the algorithm can be used for different resolution

The reproducibility of the Echo-Index has been proved as well-acceptable in general considering inexperience in neurosonology of both of the observers. The Echo-Index does not evince significant difference in case of the same image analyzed by each observer; each of them draws ROI slightly in different shape. Table 1 shows an example of computed Echo-Index for 22 images between 2 observers; there are no significant differences due to similarly drawn ROI manually by each observer.

Some images from the set were also analyzed by an experienced sonographer; ROI drawn precisely; and very similar values for Echo-index have been achieved.

Table 1: An example of measured Echo-Index between two observers for 15 randomly selected images

Image ID	Echo-Index 1	Echo-Index 2
100027	1229.35	1333.48
105520	1299.29	1371.01
128207	2036.73	1836.71
131283	1386.88	1385.05
137930	962.85	1303.37
144329	977.41	798.63
146994	1180.13	1361.27
153036	774.99	847.06
159463	1464.88	1458.29
160177	1351.90	1318.61
160507	1330.93	1476.99
162265	484.23	493.64
163803	450.52	501.71
197476	747.57	825.111
198052	570.93	653.80

2.2 Basic statistical analysis of computed Echo-Index values

To evaluate the Echo-Index reproducibility, the following statistical descriptors were analyzed from 286 B-images:

- range, variance for Echo-Index values measured by observer1 - first measurement R_{11}, var_{11}
- range, variance for Echo-Index values measured by observer1 - second measurement R_{12}, var_{12}
- range, variance for Echo-Index values measured by observer2 - first measurement R_{21}, var_{21}
- range, variance for Echo-Index values measured by observer2 - second measurement R_{22}, var_{22}
- maximum and mean difference between two observers $max(obs)$, $mean(obs)$
- correlation coefficient between Echo-Index values from 2 observers r_{obs}
- maximum and mean difference between measured values from observer1 between two weeks $max(obs1_{2w})$
- maximum and mean difference between measured values from observer2 between two weeks $max(obs2_{2w})$
- correlation coefficient of the Echo-Index values from observer1 between 2 weeks r_{obs1}
- correlation coefficient of the Echo-Index values from observer2 between 2 weeks r_{obs2}

Table 2: Basic statistical analysis to reproducibility assessment.

variable	value(s)
R_{11}, var_{11}	2423.65, 160215.98
R_{12}, var_{12}	2804.90, 164459.53
R_{21}, var_{21}	2215.96, 158765.22
R_{22}, var_{22}	2855.31, 162005.70
$max(obs)$	281.90 (absolute value)
$mean(obs)$	59.93
r_{obs}	0.947
$max(obs1_{2w})$	312.44 (absolute value)
$max(obs2_{2w})$	279.61 (absolute value)
$mean(obs1_{2w})$, $mean(obs2_{2w})$	64.72, 70.17
r_{obs1}, r_{obs2}	0.894, 0.912

Obtained results are summarized in Table 2.

Maximum values are stated in absolute value because the difference of the Echo-Index between observers or measurement can be also negative. In the case of measurement during the first phase (week), for 220 values from 278, i.e. 79.1 %, the difference under 100 between observers has been achieved. In the case of the second phase, for 214 values from 278, i.e. 76.9 %, the difference under 100 between observers has been achieved. Due to achieved results, the Echo-Index can be considered as well-reproducible value between 2 independent, non-experienced observers and also between 2 measurements from the same observer.

2.3 Echo-Index Related to Real Echogenicity Grade From Visual Assessment

In general, the basic idea "smaller Echo-Index means lower echogenicity" which was not confirmed from the point of view of an experienced sonographer, who compared images with different plaque risk level in which different echogenicity grade is obvious and there is no significant correlation between visual assessment and computed Echo-Index.

2.4 The idea of decision-making system to risk assessment based on Echo-Index value

Although the Echo-Index seems like a reproducible value, it must be thoroughly examined if the value corresponds with visual assessment by an experienced sonographer. The idea is to create a decision-making expert system using a knowledge base of echogenicity grades determined by experienced sonographer. In the future, the decision-making system can be developed to use as a tool to evaluate the probability risk of the plaque in accordance with Echo-index value in determined intervals. A draft of the system were presented in [9]. Some real case studies to use

ultrasound imaging to judge risk level of the atherosclerosis are summarized in [10].

3 Active Contour to Detect The Plaque

This part of the paper is focused on automatic selection of the ROI instead of manual process. A manual selection of the plaque is used up to now. However, each selection of the plaque takes up to 2 minutes, see in Fig. 2 that some shapes are relatively simple but another one are very complex to its exact selection.

We need to find a way how to select the plaque from the input B-image (Fig. 3) automatically. The idea is based on removing the black solid background; B-image can be comprised of the background in the major. Put differently, it is desired to detect edges of the plaque to select the Region of Interest in which the Echo-Index is computed. The active contour algorithm is one of the segmentation techniques which is used to detect the background and to extract the foreground of the image. It is based on the iterative process. In many recent studies were demonstrated that active contour segmentation technique is well applicable for medical images against its complex morphological structure. One of many studies focused on using active contour segmentation in clinical image processing is available in [7].

The goal of the active contour is to remove the black background and to extract the border of the plaque. See in Fig. 1. As a result, the goal is to execute the steps 1 to 3 automatically. The algorithm is based on iterative steps to acquire the edge which separates segmented objects in the image.

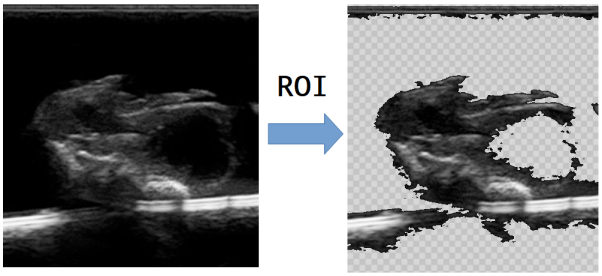

Figure 3: The idea of using segmentation principle to select the plaque border

There are two main limitations to discuss:

1. how to detect inner black areas (Fig. 1 right)
2. how to separate the plaque from the bottom of the tube
3. how to select a closed boundary as a mask ROI

The sensitivity is the primary parameter; how sensitive the detection is. Thus, what is considered as background and what is considered as foreground bordered by the edge. For example, we tried to segment the plaque using threshold level segmentation with 3 different thresholds ($T = 15$, $T = 25$ and $T = 40$). You can see in Fig. 4 that higher threshold level has the influence on segmented area.

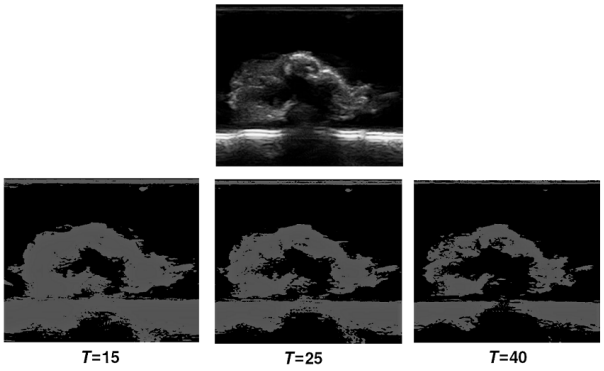

Figure 4: Three threshold levels to segment the plaque

In the case of $T = 40$, the plaque is segmented as isolated object with no bottom of the tube. To get an optimal result, the threshold is important. In the case of active contour, the number of iterations is an important parameter like the threshold. At the beginning, initial mask is set and increasing of iterations produces better border of the object.

3.1 Using Active Contour

In Fig, 4 is demonstrated that after thresholding there are many isolated objects with small area. We need to create a ROI mask which is one closed boundary (one segmented object). Using Active Contour could be a useful way to perform it.

Initially, ACM with 25 iterations has been performed. See Fig. 5 in which the results are demonstrated for 2 different images.

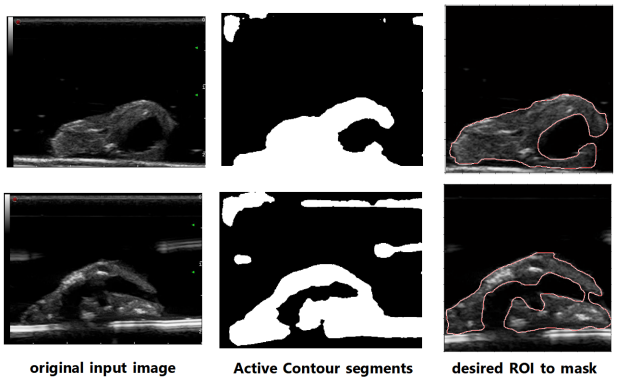

Figure 5: Using ACM with 25 iteration to detect segmented regions

The results can be used in general but as an experimental study to further improvement. Firstly, we need to sepa-

rate the plaque from the tube bottom. See Fig. 6 for some examples of the segmented masks.

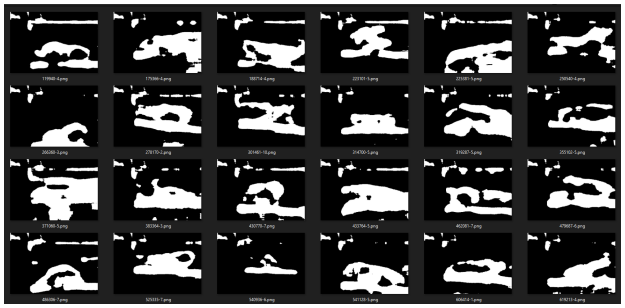

Figure 6: Example of using ACM with 25 iterations to segment atherosclerotic plaques

Surely, we can increase the number of iterations in the algorithm but no one object is get. When higher number of iterations is used, the border is get more precisely but still more than one segment is obtained.

3.2 Area Detection Using Clickable Input

Better results of the ACM were achieved with semi-automatic input. After selection of the window with the plaque, click into the plaque to understanding which segment is useful for us and set the threshold level (as H intensity level). This level is automatically computed by Otsu algorithm which can be well applicable as a segmentation method for medical images, for example in a study from 2012 [11]. The principle of the ACM is to find gradient to separate edges and the background. In Fig. 8 a magnified segment in which the border between plaque is displayed. If we can set the threshold H, the sensitivity can be adjusted; which H is the lowest value of the background.

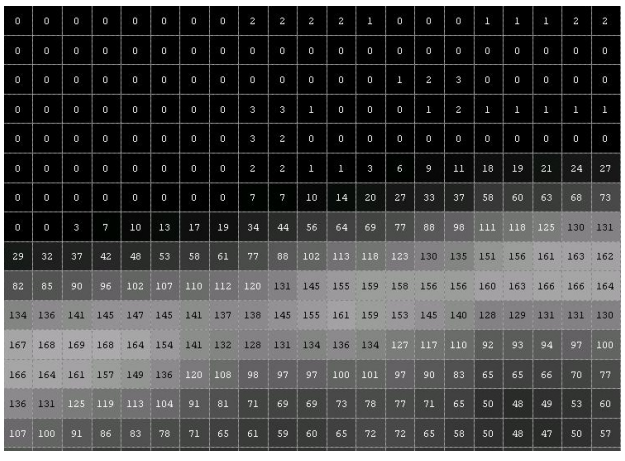

0	0	0	0	0	0	0	0	2	2	2	2	1	0	0	0	1	1	1	2	2
0	0	0	0	0	0	0	0	0	0	0	0	0	0	0	0	0	0	0	0	0
0	0	0	0	0	0	0	0	0	0	0	0	0	1	2	3	0	0	0	0	0
0	0	0	0	0	0	0	0	3	3	1	0	0	0	1	2	1	1	1	1	1
0	0	0	0	0	0	0	0	3	2	0	0	0	0	0	0	0	0	0	0	0
0	0	0	0	0	0	0	0	2	2	1	1	3	6	9	11	18	19	21	24	27
0	0	0	0	0	0	0	0	7	7	10	14	20	27	33	37	58	60	63	68	73
0	0	3	7	10	13	17	19	34	44	56	64	69	77	88	98	111	118	125	130	131
29	32	37	42	48	53	58	61	77	88	102	113	118	123	130	135	151	156	161	163	162
82	85	90	96	102	107	110	112	120	131	145	155	159	158	156	156	160	163	166	166	164
134	136	141	145	147	145	141	137	138	145	155	161	159	153	145	140	128	129	131	131	130
167	168	169	168	164	154	141	132	128	131	134	136	134	127	117	110	92	93	94	97	100
166	164	161	157	149	136	120	108	98	97	97	100	101	97	90	83	65	65	66	70	77
136	131	125	119	113	104	91	81	71	69	69	73	78	77	71	65	50	48	49	53	60
107	100	91	86	83	78	71	65	61	59	60	65	72	72	65	58	50	48	47	50	57

Figure 7: Brightness value rapidly changes between the object and the background

In Fig. 8 there are results after for $H = 20$ and click into the plaque. The results are more accurate in comparison with using ACM for the whole image.

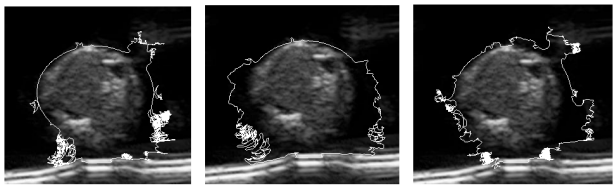

Figure 8: The results of the ACM after click the area and set the threshold

In Fig. 9 initial rectangle ROI and segmented area using ACM after only 10 iterations is shown.

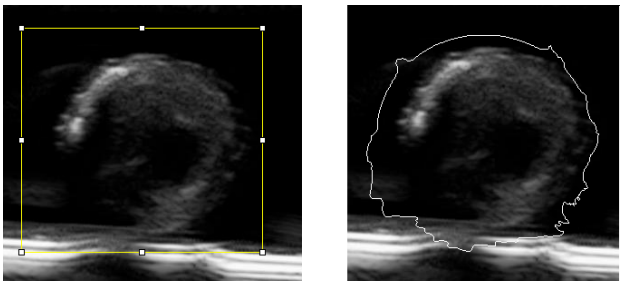

Figure 9: Initial rectangle ROI (left) selected and ACM result after 10 iterations (right)

3.3 Brightness Transformation (Contrast Enhancement) As A Pre-processing Phase

B-images have a complex structure with a lot of isolated pixels caused by noise and artifacts, see Fig. 7. To faster and more accurate results of ACM, the brightness enhancement can be recommended as a pre-processing phase at the beginning. The idea is to "clear" image from isolated pixels and enhance the brightness to better finding the contour. Let H to be brightness of the pixel. For example, all pixels with $H < 20$ can be set as $H = 0$ (as the background) and all pixels with $H > 80$ are transformed as $H + 30$. The effect is presented in Fig. 10.

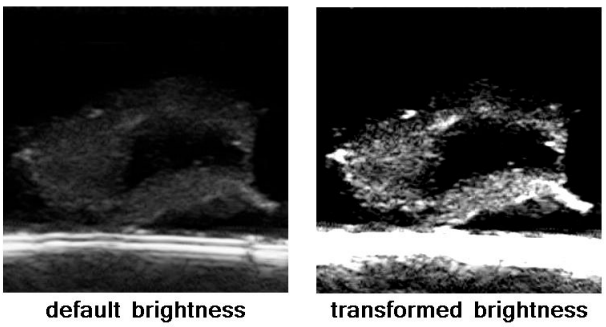

Figure 10: Brightness transformation to enhance contours to achieve faster and more accurate ACM results

The main benefit of this transformation is to eliminate noise in low echogenicity levels but some image artifacts

are enhanced too. Although it can be useful pre-processing phase to achieve better ACM results.

4 Adaptation of Active Contour Using A Convolutional Neural Network

Due to limitations mentioned above, the algorithm should be adaptable to find an appropriate border of the plaque. The result of the active contour algorithm depends primarily on brightness of the image. In other words, it is necessary to adapt the algorithm to achieve the best sensitivity in accordance with brightness of the input image. Using a neural network is one of the ideas how to improve border finding. In 2018, we published a pilot study with an experimental draft of a feed-forward neural network to recognize the shape of the plaque using edge detection operators [9]. The approach using CNN is different, based on feature recognition from a training set. The principle of the convolution mask is designed to extract some features. Earlier, we also implemented a simple neural net to detection of the ROI of substantia nigra based on training and learning of the coordinates of the ROI to put the elliptical ROI mask [6].

The goal of the CNN is to train and to learn the shape of the plaque using active contour algorithm; in other words to estimation of the active contour properties to find the best contour of the plaque in B-image. In image processing, CNN represent an eminently suitable tool for automatic segmentation using deep learning, not only for medical images.

The idea is inspired from the research [12] in which CNN are used to adaptive learning of the active contour parameters. In this case, the CNN which sets the threshold and the desired segmented area could be designed. According to complex structure of B-images, deep learning methods can be applied with CNN which are designed to extract feature maps for segmentation.

4.1 What We Expect from Using CNN

CNN should work as a supervised learning model. Therefore, we can use correctly drawn borders for training and learning process of the CNN. The convolutional layer of the CNN is designed to extract the features using a convolution kernel operation, e.g. 5×5. In Fig. 11 a simplified model of CNN is illustrated. The convolutional layer is based on computing 2-D convolution. Let $f(x,y)$ is an input image, $g(x,y)$ to be an output image and the ω to be the convolution kernel, 2-D convolution is computed by

$$g(x,y) = \omega \times f(x,y) \tag{3}$$

on 2-D image. There are usually more than one convolutional layer in CNN to detect edges, gradient to higher level of segmented objects.

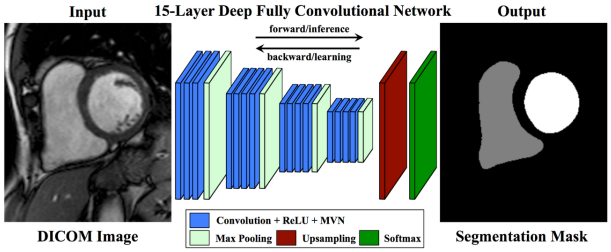

Figure 11: An example of the simplified CNN model with layers to extract segmented mask (source: https://awesomeopensource.com/project/vuptran/cardiac-segmentation

In Fig, 11 there is an example of the process what we need. No classification of the object is necessary, only to extract the mask to learn ACM model.

Design of the CNN is nontrivial, long-term process due to complexity of B-images. The goal is to interconnect the CNN with ACM algorithm to reliable detection of the plaque separately from neighbor objects (bottom of the tube). To training and learning, correct examples of plaque borders will be used. Interconnection with ACM could automatically help predict number of iterations to achieve better segmentation results of the plaque. Design, training, learning and testing of CNN are time-consuming tasks for which we need a large dataset.

4.2 Automatic ROI selection Related To Echo-Index Accuracy

Although automatic ROI selection is useful and faster, there is one meaningful relation between ROI and computed Echo-Index. To Echo-Index computing, currently only manual selection of the ROI is used. So, each ROI was precisely selected, and the difference between observers was minimal. In the case of automatic selection, ROI can be selected inaccurately in comparison with manual border drawing so Echo-Index could be different. Observe the example in Fig. 12 between manual and ACM-based border. In the case of ACM, ROI is selected including black background inside; it is undesirable. Currently, manual selection is more accurate but this a starting point to develop the ACM boosted by CNN to create an automatic segmentation of the plaque.

Due to this fact, the goal is minimize difference between manual drawing and using ACM with trained CNN to optimize the accuracy. Using CNN could predict an optimal number of iterations from training set of correctly selected ROI.

5 Conclusions, Motivation to Improve and Future Work

This paper is divided into two main parts. The first one is focused on reproducibility of the Echo-Index between

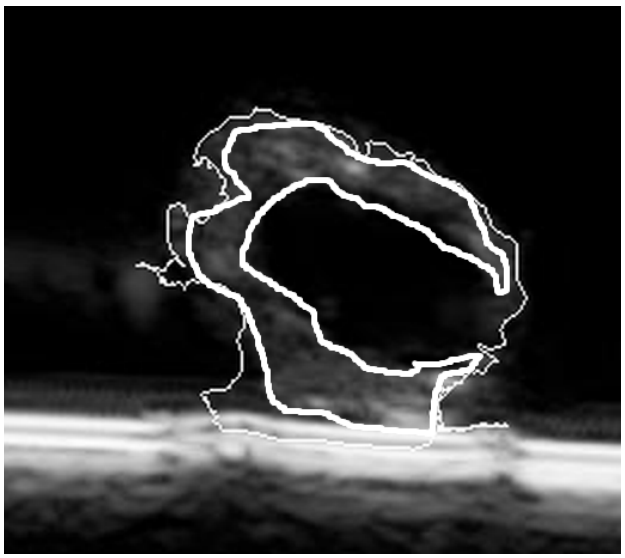

Figure 12: Manual selection is more accurate with no black area inside (bold border) in comparison with ACM-based computed ROI (light border)

two non-experienced observers for atherosclerotic plaques in B-images. In all images, the plaque was selected manually.

In the second part, the approach to automatic plaque selection instead of manual drawing the border, is discussed. Using active contour segmentation algorithm with possibility to improve the accuracy using a convolutional neural network (CNN) could be useful.

In general, the Echo-Index can be considered as a well-reproducible value. From achieved statistical results between two non-experienced observers in sonography, there is no significant difference. However, Echo-Index is not usable from the clinical point of view because there is satisfactory correlation between Echo-index and visual assessment of the echogenicity grade which should be an indicator of the risk level in general. So, lower Echo-Index value does not correspond to lower echogenicity and vice versa.

The second part is dedicated to automatic ROI selection to eliminate manual drawing the border. Currently, it is only idea to do it. It seems that using active contour algorithm could be useful. In addition, it can be supported by CNN to smart adaptation of the ACM parameters. However, this is time-consuming task to effective learn the CNN. It is one of the key goals for future work to improve automatic detection of the atherosclerotic plaque without manual drawing of the border. Faster and reliable solution using artificial intelligence components is expected.

This research is supported by the project IT4Innovations Excellence in Science - LQ1602 and data supported by Ministry of Health of the Czech Republic, grants nr. 16-28628A.

References

[1] Azar, R.N., Donaldson, C. Ultrasound Imaging (Radcases) (1st Edition) Kindle Edition. Thieme, 2014, ASIN: B00SRLKPOU.

[2] Laszlo, C., Baracchini, C. Manual of Neurosonology. Cambridge University Press; 1st Edition, 2016, ISBN-13: 978-1107659155.

[3] Blahuta, J., Cermak, P., Soukup, T., Vecerek, M. A reproducible method to transcranial B-MODE ultrasound images analysis based on echogenicity evaluation in selectable ROI. (2014) International Journal of Biology and Biomedical Engineering, Vol. 8, pp. 98-106. ISSN: 19984510.

[4] Blahuta, J., Soukup, Jelinkova, M., Bartova, P., Cermak, P., Herzig, R., Skoloudik, D.:A new program for highly reproducible automatic evaluation of the substantia nigra from transcranial sonographic images. Biomedical Papers Vol. 158 Issue 4, 621–627 (2014).

[5] Skoloudík, D., Jelinkova, M., Blahuta, J., Cermak, P., Soukup, T., Bartova, P., Langova, K., Herzig, R. Transcranial Sonography of the Substantia Nigra: Digital Image Analysis. American Journal of Neuroradiology Dec 2014, 35 (12) 2273-2278; DOI: 10.3174/ajnr.A4049.

[6] Blahuta, J., Cermak, P., Soukup, T. How to Detect and Analyze Atherosclerotic Plaques in B-MODE Ultrasound Images: A Pilot Study of Reproducibility of Computer Analysis. Artificial Intelligence: Methodology, Systems, and Applications: 17th International Conference AIMSA 2016, Varna, pp.360-363.

[7] Blahuta, J., Soukup, T., Cermak, P. An Expert System Based on Using Artificial Neural Network and Region-Based Image Processing to Recognition Substantia Nigra and Atherosclerotic Plaques in B-Images: A Prospective Study. 14th International Work-Conference on Artificial Neural Networks, IWANN 2017, Cadiz, Spain, June 14-16, 2017, Proceedings, Part I. Lecture Notes in Computer Science 10305, Springer 2017, pp 236-245.

[8] Hemalatha, R.J., Thamizhvani, T.R., Babu, B., Chandrasekaran, R., Josephin Arockia Dhivya, A., Joseph, E.J. Active Contour Based Segmentation Techniques for Medical Image Analysis. Medical and Biological Image Analysis, Robert Koprowski, IntechOpen, DOI: 10.5772/intechopen.74576.

[9] Blahuta, J., Soukup, T., Skacel, J. Pilot Design of a Rule-Based System and an Artificial Neural Network to Risk Evaluation of Atherosclerotic Plaques in Long-Range Clinical Research. ICANN 2018, Lecture Notes in Computer Science book series (LNCS, volume 11140), Springer, 2018, pp. 90-100, ISSN: 978-3-030-01420-9.

[10] Steinl, D.C., Kaufmann B.A. Ultrasound Imaging for Risk Assessment in Atherosclerosis. Int J Mol Sci. 2015 May; 16(5): 9749–9769. DOI: 10.3390/ijms16059749.

[11] Bindu, H., Prasad, K. An Efficient Medical Image Segmentation Using Conventional OTSU Method. International Journal of Advanced Science and Technology. 38.

[12] Hoogi, A., Subramaniam, A., Veerapaneni, R., Rubin, L.D. Adaptive Estimation of Active Contour Parameters Using Convolutional Neural Networks and Texture Analysis. IEEE TRANSACTIONS ON MEDICAL IMAGING, Vol. 36, No. 3, March 2017, pp. 781-791.